
Invariant Causal Mechanisms through Distribution Matching

Mathieu Chevalley¹ Charlotte Bunne¹ Andreas Krause¹ Stefan Bauer²

Abstract

Learning representations that capture the underlying data generating process is a key problem for data efficient and robust use of neural networks. One key property for robustness which the learned representation should capture and which recently received a lot of attention is described by the notion of invariance. In this work we provide a causal perspective and new algorithm for learning invariant representations. Empirically we show that this algorithm works well on a diverse set of tasks and in particular we observe state-of-the-art performance on domain generalization, where we are able to significantly boost the score of existing models.

1. Introduction

Learning structured representations which capture the underlying data-generating causal mechanisms is of central importance for training robust machine learning models (Bengio et al., 2013; Schölkopf et al., 2021). One particular structure the learned representation should capture is invariance to changes in nuisance variables. For example, we may want the representation to be *invariant* to sensitive attributes such as the race or gender of an individual in order to avoid discrimination or biased decision making in a downstream task (Creager et al., 2019; Locatello et al., 2019; Träuble et al., 2021).

While learning invariant representations is thus highly important for fairness applications, it also appears in seemingly unrelated tasks such as domain adaptation (DA) and domain generalization (DG), where one aims to be invariant across the different domains (Muandet et al., 2013; Zemel et al., 2013; Ganin et al., 2016; Peters et al., 2016). For tasks such as DA and DG, invariance across domains or environments implies being invariant to the domain index, which thus is the “sensitive attribute” in this case

and typically implies a change in the distribution of the data generating process. Being invariant to the domain index is thus a proxy to being invariant to latent unobserved factors that can change in distribution.

Established approaches for enforcing invariance in the learned representation usually aim to learn a representation whose statistical distribution is *independent* of the sensitive attribute, e.g., by including an adversary during training (Ganin et al., 2016; Xie et al., 2017). As an adversary is essentially a parametric distributional distance, other approaches minimize different distribution distances, such as maximum mean discrepancy (MMD) (Louizos et al., 2017; Li et al., 2018b), or optimal transport (OT) based distances (Shen et al., 2018; Damodaran et al., 2018). To enforce independence, these methods add a regularizer to the loss that consists of the pairwise distributional distance between all possible combinations of the sensitive attribute, i.e., $\text{dist}(p(z|d), p(z|d')) \forall d, d' \in D$. As such, the complexity of the loss grows quadratically in the size of the support of the sensitive attribute, which can limit the applicability of these models when the support of D is large (Koh et al., 2021).

Despite the importance of learning invariant representations and their potential societal impact in the medical domain or fair decision making, a commonly accepted definition is still missing and most established approaches are specialized for different tasks at hand. We take first steps towards a unifying framework by viewing *invariant representation learning* as a property of a causal process (Pearl, 2009; Peters et al., 2017) and our key contributions can be summarized as follows:

- We introduce a unifying framework for invariant representation learning, which allows us to derive a new simple and versatile regularizer to enforce invariance through distribution matching. One advantage of our algorithm is that only one distributional distance between two batches needs to be computed at each step, irrelevant of the size of the support of D .
- By enforcing a softer form of invariance, our proposed method offers a new tool with a better trade-off between predictability and stability.
- Finally, we conduct a large number of experiments across different tasks and datasets, demonstrating the versatility of our framework. We obtain competitive

¹Department of Computer Science, ETH Zürich, Zürich, Switzerland ²Department of Intelligent Systems, KTH Stockholm, Sweden. Correspondence to: Mathieu Chevalley <m.chevalley97@gmail.com>.

results on the task of learning fair representations and we are able to significantly boost the performance of existing models using our proposed algorithm for the task of DG.

2. Invariant Representation Learning Across Tasks

In this section, we highlight how the learning of an invariant representation is a goal that is (implicitly) pursued in a large spectrum of machine learning tasks.

Domain Generalization The task of DG seeks to learn a model that generalizes to an unseen domain, given some domains at training time. As such, it is a very harder task as the test domain could exhibit arbitrary shifts in distribution, and the learned model is supposed to handle any *reasonable* shifts in distribution. Without any assumptions, there is little hope to obtain models that actually generalize. Nevertheless, many inductive biases and models have been proposed, which have stronger assumptions than classical empirical risk minimization (ERM) (Vapnik, 1998).

Given its similarity to DA, similar models have been proposed, and most models work for both tasks. Nevertheless, until recently (Albuquerque et al., 2019; Deng et al., 2020), theoretical justification, e.g., for minimizing the distance between pairs of latent variables coming from different domains, was missing, as results from domain adaptation assume that the test domain is observed. Without some assumptions, there exists no theoretical reasons to infer that a constant distribution of the latent variables across the training domains leads to better generalization on the test domains. Indeed, many benchmarks (Gulrajani & Lopez-Paz, 2020; Koh et al., 2021) show that it is difficult to create algorithms that consistently beat ERM across different tasks. Invariant representations for DG was first proposed by Muandet et al. (2013). This idea was then extended to use other distributional distances, such as MMD (Li et al., 2018b), Adversarial (Li et al., 2018c; Deng et al., 2020; Albuquerque et al., 2019), and Optimal Transport (Zhou et al., 2020). On the theoretical side, both Albuquerque et al. (2019) and Deng et al. (2020) attempt to give theoretical grounding to the use of an adversarial loss by deriving bounds similar to what exists in DA.

Domain Generalization and Causal Inference Many links between causal inference and domain generalization have been made, arguing that domain generalization is inherently a causal discovery task. In particular, causal inference can be seen as a form of distributional robustness (Meinshausen, 2018). In regression, one way of ensuring interventional robustness is by identifying the causal parents of Y , whose relation to Y is stable. This can be achieved by finding a feature representation such that the optimal

classifiers are approximately the same across domains (Peters et al., 2016; Rojas-Carulla et al., 2018). Unfortunately, most of these models do not really apply to classification of structured data such as images, where the classification is predominantly anti-causal and where the wanted invariance is not toward the pixels themselves but towards the unobserved generating factors. In a similar setting to ours, Heinze-Deml & Meinshausen (2021) tackle the task of image classification and propose a new model. A significant difference to our work is that they rely on the observation of individual instances across different views, i.e., the images are clustered by an ID.

Fair Representation Learning Fair representation learning can also be viewed as an invariant representation learning task. This task seeks to learn a representation that maximizes usefulness towards predicting a target variable, while minimizing information leakage of a sensitive attribute (e.g., gender, age, race). The seminal work of Zemel et al. (2013) aims at learning a multinomial random variable Z , with associated vectors v_k , such that the representation Z is fair. More recent work directly learns a continuous variable Z that has minimal information about the sensitive attribute, either through minimizing the MMD distance (Louizos et al., 2017), through adversarial training (Edwards & Storkey, 2015; Xie et al., 2017; Roy & Boddeti, 2019), or through a Wasserstein distance (Jiang et al., 2020).

3. Background in Causality

In this section, we review some necessary theoretical background that is required for the introduction of our framework and the motivation for our newly proposed algorithm. In Appendix A, we also review some distributional distances used in this work, as our main goal is to study invariant representation learning via invariant latent variable distributions.

Causality essentially is the study of cause and effects, which goes beyond the study of statistical associations from observational data. This allows to reason about the notion of *interventions*, such as a treatment in medicine. The expected effect of an intervention is in general not equivalent to statistical conditioning, which calls for a more profound understating of the data generating process that goes beyond correlations between variables. We here focus on Pearl’s view of causality (Pearl, 2009), which mainly relies on direct acyclic graphs (DAGs).

A DAG allows to represent the relations between variables, where each variable is represented by a node in the graph. Consequently, we can interpret directed edges between nodes as the existence of a causal effect from the parent node (the cause) on the child node (the effect).

Let $G = (V, E)$ be a DAG, and P be a distribution. We say

that (G, P) is a *causal DAG model* if for any $W \subset V$ we have:

$$p(x_V | do(X_W = x'_W)) = \prod_{i \in V \setminus W} p(x_i | x_{pa_i}) I(x_W = x'_W)$$

where x_{pa_i} are the parents of node i in graph G , I is the indicator function and $do(X_W = x'_W)$ denotes the intervention on the variables X_W . As we can see above, one of the properties of a causal DAG model is that the distribution factorizes according to the parents in the associated graph G .

Structural Causal Models A structural causal model (SCM) can be seen as a more expressive version of a causal DAG model. Formally, an SCM consists of a collection S of d structural assignments, one per variable:

$$X_j \leftarrow f_j(X_{pa_j}, N_j)$$

where $X_{pa_j} \in X \setminus X_j$, and N_1 to N_d are called the *noise variables* (Definition 6.2 of Peters et al., 2017). The noise variables are assumed to be jointly independent.

For causal DAG models, we defined an intervention by $p(X_V | do(X_W = x'_W))$ (sometimes also written as $p^{do(X_W = x'_W)}(X_V)$), where the value of some variables are set to a constant value. With SCMs, we can give a more precise and general definition of interventions. An intervention now consists of replacing a subset of the collection S of structural assignments by new functions. An intervention can thus consist of replacing a variable by a constant, a new random variable or even by changing the function and its arguments (i.e., its parents). The new distribution over the variables entailed by the intervened SCM is denoted by $P^{do(X_k = \tilde{f}(X_{pa_k}, \tilde{N}_k))}$ (for more details see Definition 6.8 of Peters et al., 2017).

With this definition, we can now present the important notion of *Total Causal Effect*.

Definition 3.1. (Definition 6.12 in Peters et al., 2017) We say that a variable i has a total causal effect on a variable k if and only if:

$$X_i \not\perp\!\!\!\perp X_k \text{ in } P^{do(X_k = \tilde{N}_k)}$$

for some random variable \tilde{N}_k .

A total causal effect between a variable X_k and X_i may only exist if there is a directed path from i to k in the DAG associated to our SCM. On the other hand, there may be no total causal effect between two variable even though there exists a directed path between them in the graph.

4. Invariance as the Property of a Causal Process

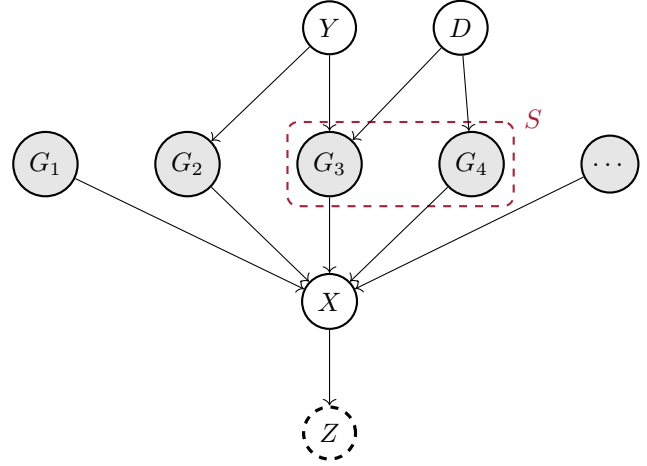


Figure 1. A DAG exhibiting our assumptions on the data generating process. We suppose that the data X is a function of unobserved generative factors G . There may exist some confounders Y and D that are parents of the generating factors. Y is the variable that we want to predict. D is the variable we want to be invariant to. Only X , D and possibly Y are observed at training time. The representation variable Z is a function of the data X that we create at training time.

In this section, we first consider the assumptions for the causal process underlying the data generating mechanism using a SCM type graph from Causality theory (Pearl, 2009) and following the causal view of learning disentangled representations (Suter et al., 2019), as illustrated in Figure 1.

G_1 to G_k represent all the factors of variation that generate the data, i.e., there exists a (one-to-one) function such that given all the factors, X is fixed: $X \leftarrow g(G_1, \dots, G_k)$.

Y is a target value that we may want to predict in a downstream task and is either known (supervised setting) or unobserved (unsupervised). D is another confounder that we want to be invariant to. It can be a domain index, such as in DA and DG, or a sensitive attribute such as in fairness. We will assume for now that D does not have an effect on Y .

Lastly, the generative factors G_i are assumed to not have any causal relations between them, and any correlation between some factors may only come from a hidden confounder. This assumption is similar to the assumptions of Suter et al. (2019). Furthermore, in this work, we assume that the label Y and D directly have an effect on the latent generating factors. In this setting, Y and D are thus independent.

Given our data generating framework, we can now give some definitions, especially the notion of style generating factors.

Definition 4.1. We call *style variables* the set of variables G that are children of D in the DAG. We denote this set S .

Remark 4.2. X and Z are independent from D given S , as they are d -separated from D by the set S in the graph. This implies that independence to D is a necessary condition for Z to be independent from S .

In this work, we propose and use the following definition of an invariant representation:

Definition 4.3. We say that a representation Z is *invariant* to a variable D if and only if D has no total causal effect on Z (Definition 3.1).

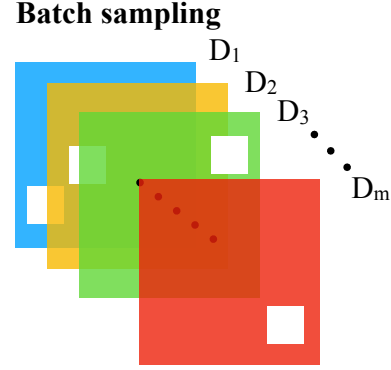
The goal of invariant representation learning can then be described as creating a new variable $Z = f(X)$ such that D has no total causal effect on Z . In a way, we can view it as adding a new variable in the SCM and learning its structural equation.

Remark 4.4. Invariance of Z from D can be enforced in two equivalent ways: either $p^{do(D=d)}(Z) = p(Z|D=d)$ to be constant for all d (as D has no causal parents in our graph, intervention is equivalent to conditioning), or $p^{do(D=\tilde{N}_D)}(Z) = \int p(Z|D=d)\tilde{N}_D(d)dd$ to be constant for all \tilde{N}_D . That is, we can enforce invariance through hard or soft interventions on D .

By being invariant to D , we are implicitly trying to be invariant to the style variables S , whose distributions are unstable. We argue that there thus exists a trade-off between predictive power of the representation and invariance, which comes from the fact that some generative factors are children of both Y and D . Being strongly invariant to D (and S) may then be detrimental to performance. This is likewise indicated in recent other works from the causality literature which show the benefits of models which trade-off stability and predictiveness (Basu et al., 2018; Pfister et al., 2019; 2021; Rothenhäusler et al., 2021) over models which are only purely focused on achieving invariance (Peters et al., 2016).

5. An Algorithm for Invariant Latent Variable Distributions

Based on the underlying assumptions of Figure 1 and Remark 4.4, we present a new algorithm to learn a representation invariant to soft interventions on D . This algorithm could be useful for example when we have a large number of different values of D , where enforcing an invariant $p(z|d)$ is hard to optimize (pairwise distances between distributions). Instead, we change the distribution of D across batches (simulated soft intervention) and take the distribution distance between pairs of batches. We formulate the optimization



a) Traditional Regularization

$$R = \text{dist}(\text{blue}, \text{yellow}) + \text{dist}(\text{blue}, \text{green}) + \dots + \text{dist}(\text{green}, \text{red})$$

b) Our Regularization

$$R = \text{dist}(\text{green-yellow-red}, \text{blue-green-red})$$

↙ ↘
New random mixtures at each step

$$\text{Loss} = \mathcal{L}(\text{blue}, \text{yellow}, \text{green}, \dots, \text{red}) + \lambda \cdot R$$

Figure 2. Visual representation of our proposed algorithm and regularization. For $\lambda = 0$, we recover traditional ERM. To compute the regularization, any distributional distances (dist in the figure) can be used. See Appendix A for a review of possible distances. At each step of optimization, batches (colored squares) are drawn for each value of D (e.g. from each domain). Those batches are then encoded and a distance between latent codes is computed for the regularization R . Traditionally, the regularization R is computed by taking the distance between pairs of batches of latent codes coming from different domains. Instead, we propose to compute R by taking only one distance between mixtures of latent codes coming from different domains. The distribution of the mixtures is changed at each step.

goal as follows:

$$\begin{aligned} \min_{Z=f(X)} \mathcal{L}(Y, c(Z)), \\ \text{s.t. } p(Z) = \text{const } \forall N_d. \end{aligned} \quad (1)$$

Now, let Q be a probability measure with full support over distributions N_d that have full support over D . We reformulate Equation (1) as follows:

$$\begin{aligned} & \min_{Z=f(X)} \mathcal{L}(Y, c(Z)), \\ \text{s.t. } & \mathbb{E}_{N_d, N'_d \sim Q} \left[\text{dist}(p^{do(d=N_d)}(Z), p^{do(d=N'_d)}(Z)) \right] = 0, \end{aligned} \quad (2)$$

where dist is a distance between distributions (see Section 3 for possible distances), and N_d, N'_d are interventions on the distribution of d drawn from Q .

For infinite data, the two constraints are equivalent: the first constraint trivially implies the second. For the other direction, the expectation being 0 implies $\text{dist}(p^{do(d=N_d)}(Z), p^{do(d=N'_d)}(Z)) = 0$ almost surely, as a distance function is non-negative. Lastly, there always exists a solution f that satisfies the constraint, e.g. $f(x) = c \forall x$, with $c \in \mathbb{R}$.

We then relax this constraint by taking the dual formulation:

$$\begin{aligned} & \min_{Z=f(X)} \mathcal{L}(Y, c(Z)) + \\ & \lambda \cdot \mathbb{E}_{N_d, N'_d \sim Q} \left[\text{dist}(p^{do(d=N_d)}(Z), p^{do(d=N'_d)}(Z)) \right]. \end{aligned} \quad (3)$$

This algorithm gives us a new method to learn invariance. Furthermore, as we minimize the average distance between soft interventions, we intuitively impose a softer regularization than taking a distance between hard interventions. This may lead to models that exhibit a better trade-off between invariance and predictive power of the representation.

Algorithm 1: Our algorithm for invariant representation learning.

```

1 Let  $d$  be the number of domains;
2 Let  $n > 0$  be the number of samples drawn from
  each domain at each step;
3 begin
4   Draw a batch  $b_i$  of  $n$  samples for each domain;
5    $B1, B2 \leftarrow \emptyset, \emptyset$ ;
   // We create two batches  $B1$  and
   //  $B2$  that approximate the
   // interventions  $N_d$  and  $N'_d$  of
   // Equation (3)
6   for  $i \leftarrow 1$  to  $d$  do
7      $s \sim \mathcal{U}(0, n)$ ;
8      $B1, B2 \leftarrow (B1, b_i[:s]), (B2, b_i[s:]);$ 
     // Concatenate  $B1$  and  $B2$  with
     // a slice of  $b_i$ 
9   end
10   $Z1, Z2 \leftarrow f(B1), f(B2)$ ;
11   $loss \leftarrow \text{dist}(Z1, Z2)$ ;
12  return  $loss$ ;
13 end
    
```

6. Empirical Evaluation

6.1. Synthetic Experiment

We first conduct a simple synthetic experiment to verify that our algorithm effectively enforces invariance to D in a setting that exactly follows our assumptions. We also simplify the setting by considering that we directly observe the generative factors.

The distribution is generated by the following set of structural equations:

$$\begin{aligned} Y & \leftarrow N_y; \\ D & \leftarrow N_d; \\ G_1 & \leftarrow Y + N_{G_1}; \\ G_2 & \leftarrow 2 \cdot Y + 2 \cdot D + N_{G_2}; \\ G_3 & \leftarrow D + N_{G_3}; \end{aligned}$$

where N_y and $N_d \sim \text{Ber}(0.5)$, $N_{G_i} \sim \mathcal{N}(0, 1)$. To create a dataset, we draw 1000 samples from our synthetic distribution and use 200 of them as test samples.

We then learn a representation that is invariant to D and that is predictive towards Y using our proposed loss. As a distributional distance, we use the MMD loss with Gaussian kernel. The architecture of the encoder is a neural network with one hidden layer of size 10 and a representation size of 5. The hidden layer is followed by a batch normalization and a ReLU activation. We use a batch size of 64 and train with the Adam optimizer (Kingma & Ba, 2015) for 200 epochs, with a learning rate of 0.001 and weight decay of 5×10^{-5} .

After training the encoder, we freeze it and train two one layer linear discriminators: one to predict Y and one to predict D . For each discriminator, we report the best achieved test accuracy. We run this experiment three times for each value of regularization $\lambda \in \{0.0, 0.1, 0.5, 1.0, 5.0, 10.0\}$. The results are summarized in Figure 3.

As expected, we can observe a strong correlation between the strength of regularization and the strength of invariance. We achieved perfect invariance with $\lambda = 10.0$, where the adversary accuracy is 50%, but target accuracy is only 54.2%. This is expected: as Y and D are strongly correlated, removing information on D in the representation also reduces the predictive power of the representation. There thus is a trade-off between performance and invariance that can be controlled via the value of λ . Finally, this experiment confirms that our proposed algorithm is a viable new method to enforce invariance.

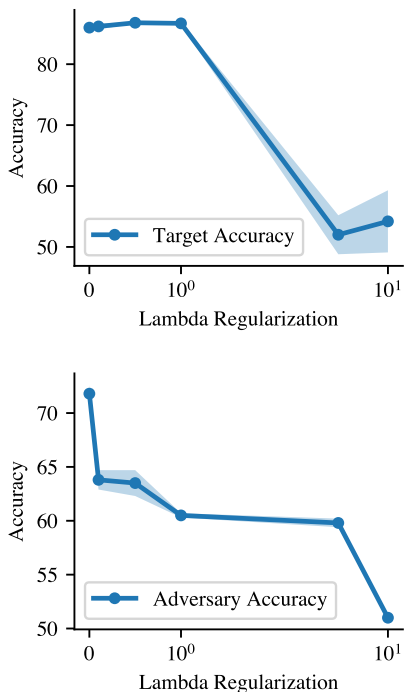


Figure 3. Graphical visualization of our results on the synthetic dataset. We can observe the trade-off between invariance (Adversary Accuracy) and performance (Target Accuracy) for different values of λ .

6.2. Fair Representation Learning experiments

We next present some experiments on fair representation learning. Here, we want to show that: (i) Fair representation learning is also an invariant representation learning task, and it is covered by our unifying framework; (ii) Our algorithm is applicable to a wide range of tasks, as it also gives competitive results on this task; (iii) Fair representation learning datasets probably also follow our proposed data generation graph.

In the context of fair representation learning, the variable D we want to be invariant to here corresponds to what is usually referred to as the *sensitive* variable. A sensitive variable is a variable that should not have an effect on the predictions of a classifier or regressor. Some examples are the sex, the race or the age of an individual. If we can construct a representation that does not contain information about the sensitive variable, there is no way for a model built on top of this representation to base its prediction on the sensitive variable. Unfortunately, in many datasets, the sensitive variable is actually predictive for the target variable, i.e., the value we are trying to predict. This introduces a trade-off between fairness and accuracy of a model.

Datasets We run experiments on two datasets from the UCI ML-repository (Asuncion & Newman, 2007), the Adult and German dataset. The German dataset seeks to predict whether an individual has good or bad credit, while the sensitive attribute is the gender. The Adult dataset aims to predict whether the annual income of an individual is more or less than 50,000\$, and the sensitive attribute is the gender. A fair model should have a sensitive accuracy that is close or below the size of the majority sensitive class, while having a target accuracy as high as possible.

Experiment Design To run our experiments, we reuse the code from Roy & Boddeti (2019) and add our model. We also empirically modify the default latent representation size such that it is optimizable using the MMD distance. As for the synthetic experiment, after training the encoder, we freeze it and learn two discriminators: one for the target and one for the sensitive attribute. The target discriminators is trained for 100 epochs and the adversary discriminator for 150 epochs. We keep the best achieved test accuracy. The goal of this setup is to assess how much information can be extracted from the representation regarding the target and sensitive variables. In Appendix B, results for the German dataset as well as figures for both datasets representing the trade-off between performance and invariance can be found.

Results (Adult Dataset) The encoder is a neural network with one hidden layer of size 7, and a latent representation size of 2. It is trained for 150 epochs using the Adam optimizer (Kingma & Ba, 2015), with learning rate 1×10^{-4} and weight decay 5×10^{-2} . The discriminators are two-hidden-layer neural networks, with hidden layers of size 64 and 32. Both are optimized using Adam with learning rate of 0.001 and weights decay of 0.001. The learning rate of the discriminators is adjusted with Cosine Annealing. Train batch size is set to 128 and test batch size to 1000.

Results are summarized in Table 1. Compared to other baselines, our best model performs well, as it has the best target accuracy for a slightly higher adversary accuracy. This shows that our method may offer a better trade-off as it allows for better performance for slightly lower invariance.

6.3. Domain Generalization

Datasets For this experiment, we test on seven datasets: ColoredMNIST (Arjovsky et al., 2019), RotatedMNIST (Ghifary et al., 2015), VLCS (Fang et al., 2013), PACS (Li et al., 2017), OfficeHome (Venkateswara et al., 2017), TerraIncognita (Beery et al., 2018) and DomainNet (Peng et al., 2019). In the Appendix, Table 6 shows sample images for each dataset under different domains and Table 7 presents each dataset’s characteristics.

Table 1. Comparison to other existing models on the Adult dataset.

MODEL	TARGET ACCURACY	ADVERSARY ACCURACY
CAUSIRL WITH MMD (OURS)	85.0	69.8
ML-ARL (XIE ET AL., 2017)	84.4	67.7
MAXENT-ARL (ROY & BODDETI, 2019)	84.6	65.5
LFR (ZEMEL ET AL., 2013)	82.3	67.0
VFAE (LOUIZOS ET AL., 2017)	81.3	67.0
MAJORITY CLASSIFIER	75.0	67.0

Experiment Design We run our experiments with the DomainBed (Gulrajani & Lopez-Paz, 2020) testbed, which is a recent widely used testbed for DG. We choose this setup as it allows for a highly fair and unbiased comparison with other existing models. DomainBed was designed to be reproducible, to give each algorithm the same amount of hyperparameter search, and to accurately estimate the variance in performance. Three model selection methods are considered: training-domain validation (all training models are pooled and a fraction of each of them is used as validation set), leave-one domain-out cross-validation (cross validation is performed using a different domain as validation, and the best models is retrained on all training domains) and test-domain validation set (a fraction of the test domain is used as validation set). The first two methods are closer to a realistic setting, whereas oracle validation allows us to evaluate whether there exists headroom for improvement. Training-domain validation assumes that all training domains and the test domain follow a similar distribution, as we pool all the training domains during training. On the other hand, leave-one domain-out cross-validation is closer to our assumption, as it optimizes for generalization to an unseen domain that is assumed to follow a different distribution.

Proposed Models We take two existing models, MMD and CORAL, based on matching distributions across domains, and propose two new models, CausIRL with MMD and with CORAL. These two new algorithms simply consist in changing how the regularization loss is computed according to our proposed algorithm, i.e., instead of taking pairwise distances across domains, we compute distances between batches that follow different domain distributions. We thus want to see if this simple change in the algorithm leads to better performance, which may be, as we conjecture, due to a better trade-off between performance and invariance, as well as the fact that it may be easier to optimize, especially in the presence of many domains. The hyperparameter λ is drawn randomly in $10^{\text{Uniform}(-1,1)}$. In the following, we present the results for two model selection methods, while the results for the last one (training-domain validation) can be found in Appendix C. Tables with comparisons to a larger number of baselines can also be found in the appendix.

6.3.1. MODEL SELECTION: LEAVE-ONE-DOMAIN-OUT CROSS-VALIDATION

We now look at the DG experiment results for the leave-one-domain-out cross-validation model selection method. The results are summarized in Table 2.

Here, the overall performance of CausIRL with CORAL is almost identical to CORAL. Nevertheless, there are some differences when looking at the performance on individual datasets. CausIRL with CORAL overperform CORAL on PACS, TerraIncognita and DomainNet, whereas CORAL performs better on VLCS and OfficeHome. However we should note that only the overperformance of CausIRL with CORAL over CORAL on DomainNet is statistically significant when looking at the confidence intervals of the average accuracies.

For CausIRL with MMD, we observe a significant boost in the overall performance compared to MMD. CausIRL with MMD performs better on almost all datasets, and we also observe a significant leap in performance on DomainNet going from 23.4% to 38.9%.

6.3.2. MODEL SELECTION: TEST-DOMAIN VALIDATION SET (ORACLE)

Finally, we here look at the DG experiment results for the test-domain validation set model selection method. The results are summarized in Table 3. This setting is less realistic as we have access to test samples during training, but it is still useful as it shows the best possible model for each algorithm. It allows us to evaluate whether there is headroom for improvement for each algorithm and to see which algorithm has the inductive bias that more closely fit the task.

For both CausIRL with CORAL and CausIRL with MMD, we observe a better overall performance compared to their vanilla counterparts. We even have that CausIRL with CORAL is the best overall performing algorithm among the evaluated algorithms. Once again, we observe a large difference in performance on DomainNet between MMD and CausIRL with MMD, going from an average accuracy of 23.5% to 40.6%. We also again have that CausIRL with CORAL is the best algorithm for DomainNet compared to all the other algorithms.

Table 2. Domain Generalization experimental results for the leave-one-domain-out cross-validation model selection method.

ALGORITHM	COLOREDMNIST	ROTATEDMNIST	VLCS	PACS	OFFICEHOME	TERRAINCOGNITA	DOMAINNET	AVG
CAUSIRL WITH CORAL (OURS)	39.1 ± 2.0	97.8 ± 0.1	76.5 ± 1.0	83.6 ± 1.2	68.1 ± 0.3	47.4 ± 0.5	41.8 ± 0.1	64.9
CORAL	39.7 ± 2.8	97.8 ± 0.1	78.7 ± 0.4	82.6 ± 0.5	68.5 ± 0.2	46.3 ± 1.7	41.1 ± 0.1	65.0
CAUSIRL WITH MMD (OURS)	36.9 ± 0.2	97.6 ± 0.1	78.2 ± 0.9	84.0 ± 0.9	65.1 ± 0.7	47.9 ± 0.3	38.9 ± 0.8	64.1
MMD	36.8 ± 0.1	97.8 ± 0.1	77.3 ± 0.5	83.2 ± 0.2	60.2 ± 5.2	46.5 ± 1.5	23.4 ± 9.5	60.7
ERM	36.7 ± 0.1	97.7 ± 0.0	77.2 ± 0.4	83.0 ± 0.7	65.7 ± 0.5	41.4 ± 1.4	40.6 ± 0.2	63.2
IRM	40.3 ± 4.2	97.0 ± 0.2	76.3 ± 0.6	81.5 ± 0.8	64.3 ± 1.5	41.2 ± 3.6	33.5 ± 3.0	62.0
GROUPDRO	36.8 ± 0.1	97.6 ± 0.1	77.9 ± 0.5	83.5 ± 0.2	65.2 ± 0.2	44.9 ± 1.4	33.0 ± 0.3	62.7
DANN	40.7 ± 2.3	97.6 ± 0.2	76.9 ± 0.4	81.0 ± 1.1	64.9 ± 1.2	44.4 ± 1.1	38.2 ± 0.2	63.4
CDANN	39.1 ± 4.4	97.5 ± 0.2	77.5 ± 0.2	78.8 ± 2.2	64.3 ± 1.7	39.9 ± 3.2	38.0 ± 0.1	62.2
VREX	36.9 ± 0.3	93.6 ± 3.4	76.7 ± 1.0	81.3 ± 0.9	64.9 ± 1.3	37.3 ± 3.0	33.4 ± 3.1	60.6

Table 3. Domain Generalization experimental results for the test-domain validation set model selection method.

ALGORITHM	COLOREDMNIST	ROTATEDMNIST	VLCS	PACS	OFFICEHOME	TERRAINCOGNITA	DOMAINNET	AVG
CAUSIRL WITH CORAL (OURS)	58.4 ± 0.3	98.0 ± 0.1	78.2 ± 0.1	87.6 ± 0.1	67.7 ± 0.2	53.4 ± 0.4	42.1 ± 0.1	69.4
CORAL	58.6 ± 0.5	98.0 ± 0.0	77.7 ± 0.2	87.1 ± 0.5	68.4 ± 0.2	52.8 ± 0.2	41.8 ± 0.1	69.2
CAUSIRL WITH MMD (OURS)	63.7 ± 0.8	97.9 ± 0.1	78.1 ± 0.1	86.6 ± 0.7	65.2 ± 0.6	52.2 ± 0.3	40.6 ± 0.2	69.2
MMD	63.3 ± 1.3	98.0 ± 0.1	77.9 ± 0.1	87.2 ± 0.1	66.2 ± 0.3	52.0 ± 0.4	23.5 ± 9.4	66.9
ERM	57.8 ± 0.2	97.8 ± 0.1	77.6 ± 0.3	86.7 ± 0.3	66.4 ± 0.5	53.0 ± 0.3	41.3 ± 0.1	68.7
IRM	67.7 ± 1.2	97.5 ± 0.2	76.9 ± 0.6	84.5 ± 1.1	63.0 ± 2.7	50.5 ± 0.7	28.0 ± 5.1	66.9
GROUPDRO	61.1 ± 0.9	97.9 ± 0.1	77.4 ± 0.5	87.1 ± 0.1	66.2 ± 0.6	52.4 ± 0.1	33.4 ± 0.3	67.9
DANN	57.0 ± 1.0	97.9 ± 0.1	79.7 ± 0.5	85.2 ± 0.2	65.3 ± 0.8	50.6 ± 0.4	38.3 ± 0.1	67.7
CDANN	59.5 ± 2.0	97.9 ± 0.0	79.9 ± 0.2	85.8 ± 0.8	65.3 ± 0.5	50.8 ± 0.6	38.5 ± 0.2	68.2
VREX	67.0 ± 1.3	97.9 ± 0.1	78.1 ± 0.2	87.2 ± 0.6	65.7 ± 0.3	51.4 ± 0.5	30.1 ± 3.7	68.2

6.4. Real-World Domain Generalization

Table 4. Performance results of our proposed models on Camelyon17 and RxRx1 compared to other baselines.

ALGORITHM	CAMELYON17	RxRx1
CAUSIRL WITH CORAL (OURS)	62.7 ± 9.4	29.0 ± 0.2
CORAL	59.5 ± 7.7	28.4 ± 0.3
CAUSIRL WITH MMD (OURS)	63.4 ± 11.2	28.9 ± 0.1
MMD	64.6 ± 10.5	28.2 ± 0.2
ERM	70.3 ± 6.4	29.9 ± 0.4
GROUPDRO	68.4 ± 7.3	23.0 ± 0.3
IRM	64.2 ± 8.1	9.9 ± 1.4

In this section, we run experiments on more realistic distributional shifts. We use the Wilds (Koh et al., 2021) benchmark and run experiments on two datasets: Camelyon17 (Bandi et al., 2018) and RxRx1 (Taylor et al., 2019). Camelyon17 consists in predicting whether a region of tissue contains tumor tissue, while being invariant to the hospitals where the sample was taken. The goal is to obtain a model that generalizes across hospitals, as hospital specific artifacts of the data collection process can vary. RxRx1 consists of cell images, where the cells received some genetic treatment (as well as no treatment). The goal is to predict the genetic treatment among 1, 139 possible treatments. Here, we want to be invariant to the batch the cells come from, as it is a common observation that batch effects can greatly alter the results.

We test our two proposed models, CausIRL with CORAL and with MMD on both datasets. For the RxRx1 dataset, we use the same hyperparameters than for the CORAL model in the Wilds implementation. For Camelyon17, we change the number of group per batch to three and the batch size

to 60. The results are summarized in Table 4. As for the DG experiments on DomainBed before, we observe that CausIRL with CORAL performs better than CORAL. Moreover, CausIRL with MMD performs slightly better than CausIRL with CORAL on Camelyon17 and similarly on RxRx1. Unfortunately, all models perform worse than simple ERM. Indeed, real world datasets exhibit far more complex data generating processes, which makes finding suitable heuristics highly difficult. Nevertheless, we again observe that our proposed models work competitively even on a realistic dataset, and that our proposed algorithm to compute the distributional distance regularization is better than how it is traditionally done.

7. Conclusion and Future Work

In this work, we provided a causal perspective on invariant representation learning. Based on this causal perspective and the assumptions on the data generating process, we then proposed a new, simple and versatile algorithm for enforcing invariance to D in the learned representations. As our regularization is softer than traditional methods, we argue that it offers a better trade-off between performance and invariance, which is supported by our empirical results. Furthermore, as our method is simple and non task specific, it should be widely applicable. As it is easily implementable, it can be a viable additional option for practitioners. Lastly, we empirically demonstrated that our algorithm is versatile as it works on a diverse set of tasks and datasets. In particular, it performs strongly in DG, where we obtain state-of-the-art performance.

References

- Albuquerque, I., Monteiro, J., Darvishi, M., Falk, T. H., and Mitliagkas, I. Generalizing to unseen domains via distribution matching. *arXiv preprint arXiv:1911.00804*, 2019.
- Arjovsky, M., Bottou, L., Gulrajani, I., and Lopez-Paz, D. Invariant risk minimization. *arXiv preprint arXiv:1907.02893*, 2019.
- Asuncion, A. and Newman, D. Uci machine learning repository, 2007.
- Bandi, P., Geessink, O., Manson, Q., Van Dijk, M., Balkenhol, M., Hermsen, M., Bejnordi, B. E., Lee, B., Paeng, K., Zhong, A., et al. From detection of individual metastases to classification of lymph node status at the patient level: the camelyon17 challenge. *IEEE Transactions on Medical Imaging*, 2018.
- Basu, S., Kumbier, K., Brown, J. B., and Yu, B. Iterative random forests to discover predictive and stable high-order interactions. *Proceedings of the National Academy of Sciences*, 115(8):1943–1948, 2018.
- Beery, S., Van Horn, G., and Perona, P. Recognition in terra incognita. *ECCV*, 2018.
- Bengio, Y., Courville, A., and Vincent, P. Representation learning: A review and new perspectives. *IEEE transactions on pattern analysis and machine intelligence*, 35(8): 1798–1828, 2013.
- Creager, E., Madras, D., Jacobsen, J.-H., Weis, M., Swersky, K., Pitassi, T., and Zemel, R. Flexibly fair representation learning by disentanglement. In *International conference on machine learning*, pp. 1436–1445. PMLR, 2019.
- Damodaran, B. B., Kellenberger, B., Flamary, R., Tuia, D., and Courty, N. Deepjdot: Deep joint distribution optimal transport for unsupervised domain adaptation. In *Proceedings of the European Conference on Computer Vision (ECCV)*, pp. 447–463, 2018.
- Deng, Z., Ding, F., Dwork, C., Hong, R., Parmigiani, G., Patil, P., and Sur, P. Representation via representations: Domain generalization via adversarially learned invariant representations. *arXiv preprint arXiv:2006.11478*, 2020.
- Edwards, H. and Storkey, A. Censoring representations with an adversary. *arXiv preprint arXiv:1511.05897*, 2015.
- Fang, C., Xu, Y., and Rockmore, D. N. Unbiased metric learning: On the utilization of multiple datasets and web images for softening bias. *ICCV*, 2013.
- Ganin, Y., Ustinova, E., Ajakan, H., Germain, P., Larochelle, H., Laviolette, F., Marchand, M., and Lempitsky, V. Domain-adversarial training of neural networks. *The journal of machine learning research*, 17(1):2096–2030, 2016.
- Ghifary, M., Bastiaan Kleijn, W., Zhang, M., and Balduzzi, D. Domain generalization for object recognition with multi-task autoencoders. *ICCV*, 2015.
- Goodfellow, I., Pouget-Abadie, J., Mirza, M., Xu, B., Warde-Farley, D., Ozair, S., Courville, A., and Bengio, Y. Generative adversarial nets. In Ghahramani, Z., Welling, M., Cortes, C., Lawrence, N. D., and Weinberger, K. Q. (eds.), *Advances in Neural Information Processing Systems 27*, pp. 2672–2680. Curran Associates, Inc., 2014. URL <http://papers.nips.cc/paper/5423-generative-adversarial-nets.pdf>.
- Gretton, A., Borgwardt, K., Rasch, M., Schölkopf, B., and Smola, A. A kernel method for the two-sample-problem. *Advances in neural information processing systems*, 19: 513–520, 2006.
- Gulrajani, I. and Lopez-Paz, D. In search of lost domain generalization. *arXiv preprint arXiv:2007.01434*, 2020.
- Heinze-Deml, C. and Meinshausen, N. Conditional variance penalties and domain shift robustness. *Machine Learning*, 110(2):303–348, 2021.
- Huang, Z., Wang, H., Xing, E. P., and Huang, D. Self-challenging improves cross-domain generalization. In *Computer Vision–ECCV 2020: 16th European Conference, Glasgow, UK, August 23–28, 2020, Proceedings, Part II 16*, pp. 124–140. Springer, 2020.
- Jiang, R., Pacchiano, A., Stepleton, T., Jiang, H., and Chiappa, S. Wasserstein fair classification. In *Uncertainty in Artificial Intelligence*, pp. 862–872. PMLR, 2020.
- Kingma, D. P. and Ba, J. Adam: A method for stochastic optimization. *ICLR*, 2015.
- Koh, P. W., Sagawa, S., Marklund, H., Xie, S. M., Zhang, M., Balsubramani, A., Hu, W., Yasunaga, M., Phillips, R. L., Gao, I., Lee, T., David, E., Stavness, I., Guo, W., Earnshaw, B. A., Haque, I. S., Beery, S., Leskovec, J., Kundaje, A., Pierson, E., Levine, S., Finn, C., and Liang, P. WILDS: A benchmark of in-the-wild distribution shifts. In *International Conference on Machine Learning (ICML)*, 2021.
- Krueger, D., Caballero, E., Jacobsen, J.-H., Zhang, A., Binas, J., Zhang, D., Le Priol, R., and Courville, A. Out-of-distribution generalization via risk extrapolation (rex). In *International Conference on Machine Learning*, pp. 5815–5826. PMLR, 2021.

- Li, D., Yang, Y., Song, Y.-Z., and Hospedales, T. M. Deeper, broader and artier domain generalization. 2017.
- Li, D., Yang, Y., Song, Y.-Z., and Hospedales, T. M. Learning to generalize: Meta-learning for domain generalization. In *Thirty-Second AAAI Conference on Artificial Intelligence*, 2018a.
- Li, H., Pan, S. J., Wang, S., and Kot, A. C. Domain generalization with adversarial feature learning. In *Proceedings of the IEEE Conference on Computer Vision and Pattern Recognition*, pp. 5400–5409, 2018b.
- Li, Y., Tian, X., Gong, M., Liu, Y., Liu, T., Zhang, K., and Tao, D. Deep domain generalization via conditional invariant adversarial networks. In *Proceedings of the European Conference on Computer Vision (ECCV)*, pp. 624–639, 2018c.
- Locatello, F., Abbati, G., Rainforth, T., Bauer, S., Schölkopf, B., and Bachem, O. On the fairness of disentangled representations. *arXiv preprint arXiv:1905.13662*, 2019.
- Louizos, C., Swersky, K., Li, Y., Welling, M., and Zemel, R. The variational fair autoencoder, 2017.
- Makhzani, A., Shlens, J., Jaitly, N., Goodfellow, I., and Frey, B. Adversarial autoencoders. *arXiv preprint arXiv:1511.05644*, 2015.
- Meinshausen, N. Causality from a distributional robustness point of view. In *2018 IEEE Data Science Workshop (DSW)*, pp. 6–10, 2018. doi: 10.1109/DSW.2018.8439889.
- Muandet, K., Balduzzi, D., and Schölkopf, B. Domain generalization via invariant feature representation. In *International Conference on Machine Learning*, pp. 10–18. PMLR, 2013.
- Nam, H., Lee, H., Park, J., Yoon, W., and Yoo, D. Reducing domain gap by reducing style bias, 2021.
- Pearl, J. *Causality*. Cambridge university press, 2009.
- Peng, X., Bai, Q., Xia, X., Huang, Z., Saenko, K., and Wang, B. Moment matching for multi-source domain adaptation. In *Proceedings of the IEEE International Conference on Computer Vision*, pp. 1406–1415, 2019.
- Peters, J., Bühlmann, P., and Meinshausen, N. Causal inference by using invariant prediction: identification and confidence intervals. *Journal of the Royal Statistical Society. Series B (Statistical Methodology)*, pp. 947–1012, 2016.
- Peters, J., Janzing, D., and Schölkopf, B. *Elements of causal inference: foundations and learning algorithms*. The MIT Press, 2017.
- Pfister, N., Bauer, S., and Peters, J. Learning stable and predictive structures in kinetic systems. *Proceedings of the National Academy of Sciences*, 116(51):25405–25411, 2019.
- Pfister, N., Williams, E. G., Peters, J., Aebbersold, R., and Bühlmann, P. Stabilizing variable selection and regression. *The Annals of Applied Statistics*, 15(3):1220–1246, 2021.
- Rojas-Carulla, M., Schölkopf, B., Turner, R., and Peters, J. Invariant models for causal transfer learning. *The Journal of Machine Learning Research*, 19(1):1309–1342, 2018.
- Rothhäusler, D., Meinshausen, N., Bühlmann, P., and Peters, J. Anchor regression: Heterogeneous data meet causality. *Journal of the Royal Statistical Society: Series B (Statistical Methodology)*, 83(2):215–246, 2021.
- Roy, P. C. and Boddeti, V. N. Mitigating information leakage in image representations: A maximum entropy approach. 2019.
- Sagawa, S., Koh, P. W., Hashimoto, T. B., and Liang, P. Distributionally robust neural networks for group shifts: On the importance of regularization for worst-case generalization. *arXiv preprint arXiv:1911.08731*, 2019.
- Schölkopf, B., Locatello, F., Bauer, S., Ke, N. R., Kalchbrenner, N., Goyal, A., and Bengio, Y. Toward causal representation learning. *Proceedings of the IEEE*, 109(5): 612–634, 2021.
- Shen, J., Qu, Y., Zhang, W., and Yu, Y. Wasserstein distance guided representation learning for domain adaptation. In *Proceedings of the AAAI Conference on Artificial Intelligence*, volume 32, 2018.
- Sun, B. and Saenko, K. Deep coral: Correlation alignment for deep domain adaptation. In *European conference on computer vision*, pp. 443–450. Springer, 2016.
- Suter, R., Miladinovic, D., Schölkopf, B., and Bauer, S. Robustly disentangled causal mechanisms: Validating deep representations for interventional robustness. In *International Conference on Machine Learning*, pp. 6056–6065. PMLR, 2019.
- Taylor, J., Earnshaw, B., Mabey, B., Victors, M., and Yosinski, J. Rxxr1: An image set for cellular morphological variation across many experimental batches. In *International Conference on Learning Representations (ICLR)*, 2019.
- Träuble, F., Creager, E., Kilbertus, N., Locatello, F., Dittadi, A., Goyal, A., Schölkopf, B., and Bauer, S. On disentangled representations learned from correlated data. In *International Conference on Machine Learning*, pp. 10401–10412. PMLR, 2021.

- Vapnik, V. Statistical learning theory wiley. *New York*, 1998.
- Venkateswara, H., Eusebio, J., Chakraborty, S., and Panchanathan, S. Deep hashing network for unsupervised domain adaptation. *CVPR*, 2017.
- Xie, Q., Dai, Z., Du, Y., Hovy, E., and Neubig, G. Controllable invariance through adversarial feature learning. *arXiv preprint arXiv:1705.11122*, 2017.
- Yan, S., Song, H., Li, N., Zou, L., and Ren, L. Improve unsupervised domain adaptation with mixup training. *arXiv preprint arXiv:2001.00677*, 2020.
- Zemel, R., Wu, Y., Swersky, K., Pitassi, T., and Dwork, C. Learning fair representations. In Dasgupta, S. and McAllester, D. (eds.), *Proceedings of the 30th International Conference on Machine Learning*, volume 28 of *Proceedings of Machine Learning Research*, pp. 325–333, Atlanta, Georgia, USA, 17–19 Jun 2013. PMLR. URL <http://proceedings.mlr.press/v28/zemel13.html>.
- Zhang, M. M., Marklund, H., Dhawan, N., Gupta, A., Levine, S., and Finn, C. Adaptive risk minimization: A meta-learning approach for tackling group shift. 2020.
- Zhou, F., Jiang, Z., Shui, C., Wang, B., and Chaib-draa, B. Domain generalization with optimal transport and metric learning. *arXiv preprint arXiv:2007.10573*, 2020.

A. Additional Background

A.1. Distributional Distances

The main goal of this work is to study how invariance can be enforced by regularizing different latent spaces to have the same distribution. To this end, we thus need a differentiable distance or divergence between distributions that can be minimized during training. We here present the most commonly used distances in the literature.

A.1.1. ADVERSARIAL

Adversarial training was first introduced in (Goodfellow et al., 2014) as a new method for Generative modeling. Based on game theory, it can intuitively be described as a two player game, where each player is parameterized by a neural network. The Generator is a function that maps its input distribution to an output distribution. We call it the generated distribution and denote it by p_g . On the other hand, a Discriminator tries to distinguish between samples coming from the target dataset and samples produced by the Generator. At convergence, the Generator produces data that is distributed similarly to the target distribution, and thus it becomes impossible for the Discriminator to distinguish samples.

Formally, the objective of the two-player minimax game reads:

$$\min_G \max_D V(D, G) = \mathbb{E}_{\mathbf{x} \sim p_{data}(\mathbf{x})} [\log D(\mathbf{x})] + \mathbb{E}_{\mathbf{z} \sim p_{\mathbf{z}}(\mathbf{z})} [\log (1 - D(G(\mathbf{z})))] \quad (4)$$

where \mathbf{z} is the input, \mathbf{x} comes from the target distributions, and the Discriminator D should output 1 when its input is a samples from the target, and 0 otherwise. If the Discriminator is optimal for a given G , Equation (4) can be rewritten to show that the Generator actually minimizes the Jensen–Shannon divergence (JSD) between the generated and target distribution.

$$JSD(P||Q) = \frac{1}{2} D_{\text{KL}} \left(P \left\| \frac{1}{2} (P + Q) \right. \right) + \frac{1}{2} D_{\text{KL}} \left(Q \left\| \frac{1}{2} (P + Q) \right. \right),$$

where D_{KL} is the Kullback-Leibler (KLd) divergence. It also can be shown that if both networks have sufficient capacity, and if the Discriminator is trained to optimality after each optimization step of the Generator, then the distribution of the Generator converges to the target distribution.

Adversarial training can thus be seen as a proxy distributional distance, which corresponds to the JSD at convergence. This concept of adversarial training has been extended to be used as a regularizer for latent spaces. It can for example be used to enforce a prior distribution on the latent space (Makhzani et al., 2015). It can also be used to enforce two latent spaces to have the same distribution. Its use is often justified as wanting two latent spaces to seem *indistinguishable* for an adversary, which is supposed to force the encoder to discard what is not constant across the two input distribution. We argue that adversarial training is theoretically equivalent to minimizing any distributional divergence, and that only their optimization properties differentiate them. We will also later clarify the intuition of trying to discard the *idiosyncratic in favor of the universal*, and what it actually corresponds to when we look at the data generation process of a given dataset.

A.1.2. MAXIMUM MEAN DISCREPANCY

MMD (Gretton et al., 2006) is a distance based on empirical samples from two distributions, based on the distance between the means of the two sets of samples mapped into a reproducing kernel Hilbert space (RKHS). Let $\{X\} \sim P$ and $\{X'\} \sim Q$. Then, we have:

$$\begin{aligned} MMD(X, X')^2 &= \left\| \frac{1}{n} \sum_{i=1}^n \phi(x_i) - \frac{1}{n'} \sum_{i=1}^{n'} \phi(x'_i) \right\|^2 \\ &= \frac{1}{n^2} \sum_{i,j=1}^n k(x_i, x_j) + \frac{1}{n'^2} \sum_{i,j=1}^{n'} k(x'_i, x'_j) - \frac{2}{n \cdot n'} \sum_{i=1}^n \sum_{j=1}^{n'} k(x_i, x'_j), \end{aligned}$$

where $k(\cdot, \cdot)$ is the associated kernel. One commonly used kernel is the Gaussian kernel $k(x, x') = e^{-\lambda \|x - x'\|^2}$. Asymptotically, for a universal kernel such as the Gaussian kernel, $MMD(X, X') = 0$ if and only if $P = Q$. Minimizing the MMD

distance during training can thus be used to align two distributions.

B. Fair representation learning supplements

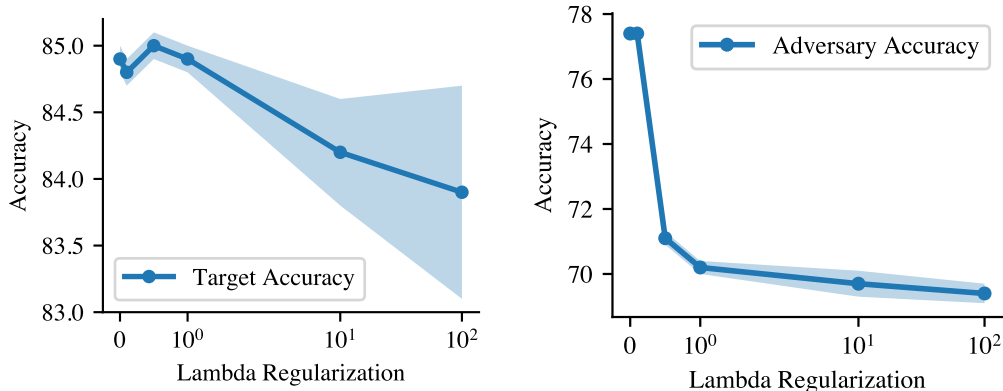


Figure 4. Graphical visualization of our results on the Adult dataset. We can observe the trade-off between invariance (Adversary Accuracy) and performance (Target Accuracy) for different values of λ .

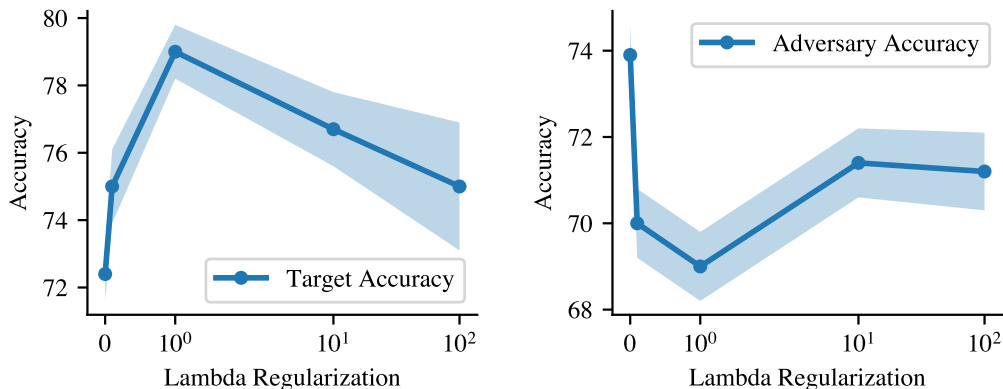


Figure 5. Graphical visualization of our results on the German dataset. We can observe the trade-off between invariance (Adversary Accuracy) and performance (Target Accuracy) for different values of λ .

German Dataset The encoder is a neural network with two hidden layers of size 15 and 8, and a latent representation size of 32. It is trained for 150 epochs using the Adam optimizer, with learning rate of 1×10^{-4} and weight decay of 5×10^{-2} . The discriminators are two-hidden-layer neural networks, with hidden layers of size 10. Both are optimized using Adam with learning rate of 0.001 and weights decay of 0.001. The learning rate of the discriminators is adjusted with Cosine Annealing. Train batch size is set to 64 and test batch size to 100.

Results are summarized in Figure 5, as well as a comparison with other baselines in Table 5. Here, we observe that 1.0 is a clear optimal value for λ , as it gives the highest target accuracy and the lowest adversary accuracy. A bit more surprisingly, we observe that higher regularization can give lesser invariance, which we can interpret as a form of over-regularization. Compared to other methods, we obtain competitive results as we get the smallest adversary accuracy, even below the majority prediction, while still obtaining the second best target accuracy.

Compute Resources We run the experiments on NVIDIA GEFORCE RTX 2080 Ti GPUs.

Table 5. Comparison to other existing models on the German dataset.

MODEL	TARGET ACCURACY	ADVERSARY ACCURACY
CAUSIRL WITH MMD (OURS)	80.3	67.0
ML-ARL (XIE ET AL., 2017)	74.4	80.2
MAXENT-ARL (ROY & BODDETI, 2019)	86.3	72.7
LFR (ZEMEL ET AL., 2013)	72.3	80.5
VFAE (LOUIZOS ET AL., 2017)	72.7	79.7
MAJORITY CLASSIFIER	71.0	69.0

C. DG supplements

Compute Resources We run the 10,560 jobs on NVIDIA GEFORCE RTX 2080 Ti GPUs as well as NVIDIA TITAN RTX GPUs for the more resource intensive jobs.

Baseline models We compare our algorithms to the following existing algorithms:

- Empirical Risk Minimization (ERM, (Vapnik, 1998)), where the sum of errors is minimized across domains.
- Group Distributionally Robust Optimization (DRO, (Sagawa et al., 2019)), where low performing domains are giving an increasing weight during training.
- Inter-domain Mixup (Mixup, (Yan et al., 2020)).
- Meta-Learning for Domain Generalization (MLDG, (Li et al., 2018a)).
- Algorithms based on matching the latent distribution across domains:
 - Domain-Adversarial Neural Networks (DANN, (Ganin et al., 2016)), where the distributional distance is an adversarial network.
 - Class-conditional DANN (C-DANN, (Li et al., 2018c)), which is a variant of DANN matching the class conditional distributions across domains.
 - CORAL (Sun & Saenko, 2016), which aligns the mean and covariance of latent distributions.
 - MMD (Li et al., 2018b), which uses the MMD distance.
- Invariant Risk Minimization (IRM (Arjovsky et al., 2019)), which looks for a representation whose optimal linear classifier on top of the representation matches across domains.
- Style Agnostic Networks (SagNet, (Nam et al., 2021)), which tries to reduce style bias of CNNs.
- Adaptive Risk Minimization (ARM, (Zhang et al., 2020)), which is based on meta-learning.
- Variance Risk Extrapolation (VREx, (Krueger et al., 2021)), where they enforce the training risk to be similar across domains.
- Representation Self-Challenging (RSC, (Huang et al., 2020)).

Implementation To be more concrete, we change the code that computes the distributional distance penalty from this:

```
for i in range(nmb):
    for j in range(i + 1, nmb):
        penalty += self.dist_loss(features[i], features[j])

if nmb > 1:
    penalty /= (nmb * (nmb - 1) / 2)
```

to this:

Table 6. Datasets used in our DG experiments, with sample images for each of them. This table is taken from (Gulrajani & Lopez-Paz, 2020).

Dataset	Domains					
Colored MNIST	+90%	+80%	-90%			
<i>(degree of correlation between color and label)</i>						
Rotated MNIST	0°	15°	30°	45°	60°	75°
VLCS	Caltech101	LabelMe	SUN09	VOC2007		
PACS	Art	Cartoon	Photo	Sketch		
Office-Home	Art	Clipart	Product	Photo		
Terra Incognita	L100	L38	L43	L46		
<i>(camera trap location)</i>						
DomainNet	Clipart	Infographic	Painting	QuickDraw	Photo	Sketch

Table 7. Description of the datasets used in our DG experiments

Dataset Name	Support of D	Number of Samples	Image Dimensions	Number of Classes
ColoredMNIST (Arjovsky et al., 2019)	{0.1, 0.3, 0.9}	70,000	(2, 28, 28)	2
RotatedMNIST (Ghifary et al., 2015)	{0, 15, 30, 45, 60, 75}	70,000	(1, 28, 28)	10
VLCS (Fang et al., 2013)	{Caltech101, LabelMe, SUN09, VOC2007}	10,729	(3, 224, 224)	5
PACS (Li et al., 2017)	{art, cartoons, photos, sketches}	9,991	(3, 224, 224)	7
OfficeHome (Venkateswara et al., 2017)	{art, clipart, product, real}	15,588	(3, 224, 224)	65
TerraIncognita (Beery et al., 2018)	{L100, L38, L43, L46}	24,788	(3, 224, 224)	10
DomainNet (Peng et al., 2019)	{clipart, infograph, painting, quickdraw, real, sketch}	586,575	(3, 224, 224)	345

```

first = None
second = None

for i in range(nmb):
    slice = random.randint(0, len(features[i]))

    if first is None:
        first = features[i][:slice]
        second = features[i][slice:]
    else:
        first = torch.cat((first, features[i][:slice]), 0)
        second = torch.cat((second, features[i][slice:]), 0)

penalty = self.dist_loss(first, second)

```

Here is the concrete full class of our CausIRL with MMD model:

```

class CausIRL_MMD(ERM):
    def __init__(self, input_shape, num_classes, num_domains, hparams):
        super(CausIRL_MMD, self).__init__(input_shape, num_classes, num_domains,
                                           hparams)
        self.kernel_type = "gaussian"

    def my_cdist(self, x1, x2):
        x1_norm = x1.pow(2).sum(dim=-1, keepdim=True)
        x2_norm = x2.pow(2).sum(dim=-1, keepdim=True)
        res = torch.addmm(x2_norm.transpose(-2, -1),
                          x1,
                          x2.transpose(-2, -1), alpha=-2).add_(x1_norm)
        return res.clamp_min_(1e-30)

    def gaussian_kernel(self, x, y, gamma=[0.001, 0.01, 0.1, 1, 10, 100,
                                           1000]):
        D = self.my_cdist(x, y)
        K = torch.zeros_like(D)

        for g in gamma:
            K.add_(torch.exp(D.mul(-g)))

        return K

    def mmd(self, x, y):
        Kxx = self.gaussian_kernel(x, x).mean()
        Kyy = self.gaussian_kernel(y, y).mean()
        Kxy = self.gaussian_kernel(x, y).mean()
        return Kxx + Kyy - 2 * Kxy

    def update(self, minibatches, unlabeled=None):
        objective = 0
        penalty = 0
        nmb = len(minibatches)

        features = [self.featurizer(xi) for xi, _ in minibatches]
        classifs = [self.classifier(fi) for fi in features]

```

```

targets = [yi for _, yi in minibatches]

first = None
second = None

for i in range(nmb):
    objective += F.cross_entropy(classifs[i] + 1e-16, targets[i])
    slice = random.randint(0, len(features[i]))
    if first is None:
        first = features[i][:slice]
        second = features[i][slice:]
    else:
        first = torch.cat((first, features[i][:slice]), 0)
        second = torch.cat((second, features[i][slice:]), 0)
    if len(first) > 1 and len(second) > 1:
        penalty = torch.nan_to_num(self.mmd(first, second))
    else:
        penalty = torch.tensor(0)

objective /= nmb

self.optimizer.zero_grad()
(objective + (self.hparams['mmd_gamma']*penalty)).backward()
self.optimizer.step()

if torch.is_tensor(penalty):
    penalty = penalty.item()

return {'loss': objective.item(), 'penalty': penalty}

```

C.1. Model Selection: Training-Domain Validation Set

We present here the results of our DG experiments for the training-domain validation model selection method. Results are summarized in Table 8. For CausIRL with CORAL, the overall performance is slightly below vanilla CORAL. CausIRL with CORAL especially underperforms CORAL on the PACS dataset. On the other hand, CausIRL with CORAL performs better than CORAL on DomainNet. For CausIRL with MMD, the overall performance is significantly better than MMD. This overperformance is mainly driven by the results on TerraIncognita and DomainNet, where for the latter we observe a leap in accuracy from 23.4% to 40.3%.

C.2. Model selection: leave-one-domain-out cross-validation

We here present the complete results for the leave-one-domain-out cross-validation model selection method in Table 9.

C.3. Model Selection: Test-Domain Validation Set (Oracle)

We here present the complete results for the test-domain validation set model selection method in Table 10.

Invariant Causal Mechanisms through Distribution Matching

Table 8. DG experimental results for the training-domain validation selection method.

Algorithm	ColoredMNIST	RotatedMNIST	VLCS	PACS	OfficeHome	TerraIncognita	DomainNet	Avg
CausIRL with CORAL (ours)	51.7 ± 0.1	97.9 ± 0.1	77.5 ± 0.6	85.8 ± 0.1	68.6 ± 0.3	47.3 ± 0.8	41.9 ± 0.1	67.3
CORAL	51.5 ± 0.1	98.0 ± 0.1	78.8 ± 0.6	86.2 ± 0.3	68.7 ± 0.3	47.6 ± 1.0	41.5 ± 0.1	67.5
CausIRL with MMD (ours)	51.6 ± 0.1	97.9 ± 0.0	77.6 ± 0.4	84.0 ± 0.8	65.7 ± 0.6	46.3 ± 0.9	40.3 ± 0.2	66.2
MMD	51.5 ± 0.2	97.9 ± 0.0	77.5 ± 0.9	84.6 ± 0.5	66.3 ± 0.1	42.2 ± 1.6	23.4 ± 9.5	63.3
ERM	51.5 ± 0.1	98.0 ± 0.0	77.5 ± 0.4	85.5 ± 0.2	66.5 ± 0.3	46.1 ± 1.8	40.9 ± 0.1	66.6
IRM	52.0 ± 0.1	97.7 ± 0.1	78.5 ± 0.5	83.5 ± 0.8	64.3 ± 2.2	47.6 ± 0.8	33.9 ± 2.8	65.4
GroupDRO	52.1 ± 0.0	98.0 ± 0.0	76.7 ± 0.6	84.4 ± 0.8	66.0 ± 0.7	43.2 ± 1.1	33.3 ± 0.2	64.8
Mixup	52.1 ± 0.2	98.0 ± 0.1	77.4 ± 0.6	84.6 ± 0.6	68.1 ± 0.3	47.9 ± 0.8	39.2 ± 0.1	66.7
MLDG	51.5 ± 0.1	97.9 ± 0.0	77.2 ± 0.4	84.9 ± 1.0	66.8 ± 0.6	47.7 ± 0.9	41.2 ± 0.1	66.7
DANN	51.5 ± 0.3	97.8 ± 0.1	78.6 ± 0.4	83.6 ± 0.4	65.9 ± 0.6	46.7 ± 0.5	38.3 ± 0.1	66.1
CDANN	51.7 ± 0.1	97.9 ± 0.1	77.5 ± 0.1	82.6 ± 0.9	65.8 ± 1.3	45.8 ± 1.6	38.3 ± 0.3	65.6
MTL	51.4 ± 0.1	97.9 ± 0.0	77.2 ± 0.4	84.6 ± 0.5	66.4 ± 0.5	45.6 ± 1.2	40.6 ± 0.1	66.2
SagNet	51.7 ± 0.0	98.0 ± 0.0	77.8 ± 0.5	86.3 ± 0.2	68.1 ± 0.1	48.6 ± 1.0	40.3 ± 0.1	67.2
ARM	56.2 ± 0.2	98.2 ± 0.1	77.6 ± 0.3	85.1 ± 0.4	64.8 ± 0.3	45.5 ± 0.3	35.5 ± 0.2	66.1
VREx	51.8 ± 0.1	97.9 ± 0.1	78.3 ± 0.2	84.9 ± 0.6	66.4 ± 0.6	46.4 ± 0.6	33.6 ± 2.9	65.6
RSC	51.7 ± 0.2	97.6 ± 0.1	77.1 ± 0.5	85.2 ± 0.9	65.5 ± 0.9	46.6 ± 1.0	38.9 ± 0.5	66.1

Table 9. DG experimental results for the leave-one-domain-out cross-validation model selection method.

Algorithm	ColoredMNIST	RotatedMNIST	VLCS	PACS	OfficeHome	TerraIncognita	DomainNet	Avg
CausIRL with CORAL (ours)	39.1 ± 2.0	97.8 ± 0.1	76.5 ± 1.0	83.6 ± 1.2	68.1 ± 0.3	47.4 ± 0.5	41.8 ± 0.1	64.9
CORAL	39.7 ± 2.8	97.8 ± 0.1	78.7 ± 0.4	82.6 ± 0.5	68.5 ± 0.2	46.3 ± 1.7	41.1 ± 0.1	65.0
CausIRL with MMD (ours)	36.9 ± 0.2	97.6 ± 0.1	78.2 ± 0.9	84.0 ± 0.9	65.1 ± 0.7	47.9 ± 0.3	38.9 ± 0.8	64.1
MMD	36.8 ± 0.1	97.8 ± 0.1	77.3 ± 0.5	83.2 ± 0.2	60.2 ± 5.2	46.5 ± 1.5	23.4 ± 9.5	60.7
ERM	36.7 ± 0.1	97.7 ± 0.0	77.2 ± 0.4	83.0 ± 0.7	65.7 ± 0.5	41.4 ± 1.4	40.6 ± 0.2	63.2
IRM	40.3 ± 4.2	97.0 ± 0.2	76.3 ± 0.6	81.5 ± 0.8	64.3 ± 1.5	41.2 ± 3.6	33.5 ± 3.0	62.0
GroupDRO	36.8 ± 0.1	97.6 ± 0.1	77.9 ± 0.5	83.5 ± 0.2	65.2 ± 0.2	44.9 ± 1.4	33.0 ± 0.3	62.7
Mixup	33.4 ± 4.7	97.8 ± 0.0	77.7 ± 0.6	83.2 ± 0.4	67.0 ± 0.2	48.7 ± 0.4	38.5 ± 0.3	63.8
MLDG	36.7 ± 0.2	97.6 ± 0.0	77.2 ± 0.9	82.9 ± 1.7	66.1 ± 0.5	46.2 ± 0.9	41.0 ± 0.2	64.0
DANN	40.7 ± 2.3	97.6 ± 0.2	76.9 ± 0.4	81.0 ± 1.1	64.9 ± 1.2	44.4 ± 1.1	38.2 ± 0.2	63.4
CDANN	39.1 ± 4.4	97.5 ± 0.2	77.5 ± 0.2	78.8 ± 2.2	64.3 ± 1.7	39.9 ± 3.2	38.0 ± 0.1	62.2
MTL	35.0 ± 1.7	97.8 ± 0.1	76.6 ± 0.5	83.7 ± 0.4	65.7 ± 0.5	44.9 ± 1.2	40.6 ± 0.1	63.5
SagNet	36.5 ± 0.1	94.0 ± 3.0	77.5 ± 0.3	82.3 ± 0.1	67.6 ± 0.3	47.2 ± 0.9	40.2 ± 0.2	63.6
ARM	36.8 ± 0.0	98.1 ± 0.1	76.6 ± 0.5	81.7 ± 0.2	64.4 ± 0.2	42.6 ± 2.7	35.2 ± 0.1	62.2
VREx	36.9 ± 0.3	93.6 ± 3.4	76.7 ± 1.0	81.3 ± 0.9	64.9 ± 1.3	37.3 ± 3.0	33.4 ± 3.1	60.6
RSC	36.5 ± 0.2	97.6 ± 0.1	77.5 ± 0.5	82.6 ± 0.7	65.8 ± 0.7	40.0 ± 0.8	38.9 ± 0.5	62.7

Table 10. DG experimental results for the test-domain validation set model selection method.

Algorithm	ColoredMNIST	RotatedMNIST	VLCS	PACS	OfficeHome	TerraIncognita	DomainNet	Avg
CausIRL with CORAL (ours)	58.4 ± 0.3	98.0 ± 0.1	78.2 ± 0.1	87.6 ± 0.1	67.7 ± 0.2	53.4 ± 0.4	42.1 ± 0.1	69.4
CORAL	58.6 ± 0.5	98.0 ± 0.0	77.7 ± 0.2	87.1 ± 0.5	68.4 ± 0.2	52.8 ± 0.2	41.8 ± 0.1	69.2
CausIRL with MMD (ours)	63.7 ± 0.8	97.9 ± 0.1	78.1 ± 0.1	86.6 ± 0.7	65.2 ± 0.6	52.2 ± 0.3	40.6 ± 0.2	69.2
MMD	63.3 ± 1.3	98.0 ± 0.1	77.9 ± 0.1	87.2 ± 0.1	66.2 ± 0.3	52.0 ± 0.4	23.5 ± 9.4	66.9
ERM	57.8 ± 0.2	97.8 ± 0.1	77.6 ± 0.3	86.7 ± 0.3	66.4 ± 0.5	53.0 ± 0.3	41.3 ± 0.1	68.7
IRM	67.7 ± 1.2	97.5 ± 0.2	76.9 ± 0.6	84.5 ± 1.1	63.0 ± 2.7	50.5 ± 0.7	28.0 ± 5.1	66.9
GroupDRO	61.1 ± 0.9	97.9 ± 0.1	77.4 ± 0.5	87.1 ± 0.1	66.2 ± 0.6	52.4 ± 0.1	33.4 ± 0.3	67.9
Mixup	58.4 ± 0.2	98.0 ± 0.1	78.1 ± 0.3	86.8 ± 0.3	68.0 ± 0.2	54.4 ± 0.3	39.6 ± 0.1	69.0
MLDG	58.2 ± 0.4	97.8 ± 0.1	77.5 ± 0.1	86.8 ± 0.4	66.6 ± 0.3	52.0 ± 0.1	41.6 ± 0.1	68.7
DANN	57.0 ± 1.0	97.9 ± 0.1	79.7 ± 0.5	85.2 ± 0.2	65.3 ± 0.8	50.6 ± 0.4	38.3 ± 0.1	67.7
CDANN	59.5 ± 2.0	97.9 ± 0.0	79.9 ± 0.2	85.8 ± 0.8	65.3 ± 0.5	50.8 ± 0.6	38.5 ± 0.2	68.2
MTL	57.6 ± 0.3	97.9 ± 0.1	77.7 ± 0.5	86.7 ± 0.2	66.5 ± 0.4	52.2 ± 0.4	40.8 ± 0.1	68.5
SagNet	58.2 ± 0.3	97.9 ± 0.0	77.6 ± 0.1	86.4 ± 0.4	67.5 ± 0.2	52.5 ± 0.4	40.8 ± 0.2	68.7
ARM	63.2 ± 0.7	98.1 ± 0.1	77.8 ± 0.3	85.8 ± 0.2	64.8 ± 0.4	51.2 ± 0.5	36.0 ± 0.2	68.1
VREx	67.0 ± 1.3	97.9 ± 0.1	78.1 ± 0.2	87.2 ± 0.6	65.7 ± 0.3	51.4 ± 0.5	30.1 ± 3.7	68.2
RSC	58.5 ± 0.5	97.6 ± 0.1	77.8 ± 0.6	86.2 ± 0.5	66.5 ± 0.6	52.1 ± 0.2	38.9 ± 0.6	68.2